

Phosphate-enabled mechanochemical PFAS destruction for fluoride reuse

<https://doi.org/10.1038/s41586-025-08698-5>

Received: 17 August 2024

Accepted: 24 January 2025

Published online: 26 March 2025

Open access

 Check for updates

Long Yang^{1,3}, Zijun Chen^{1,3}, Christopher A. Goult¹, Thomas Schlatter¹, Robert S. Paton²✉ & Véronique Gouverneur¹✉

Perfluoroalkyl and polyfluoroalkyl substances (PFASs) are persistent, bioaccumulative and anthropogenic pollutants that have attracted the attention of the public and private sectors because of their adverse impact on human health¹. Although various technologies have been deployed to degrade PFASs with a focus on non-polymeric functionalized compounds (perfluorooctanoic acid and perfluorooctanesulfonic acid)^{2–4}, a general PFAS destruction method coupled with fluorine recovery for upcycling is highly desirable. Here we disclose a protocol that converts multiple classes of PFAS, including the fluoroplastics polytetrafluoroethylene and polyvinylidene fluoride, into high-value fluorochemicals. To achieve this, PFASs were reacted with potassium phosphate salts under solvent-free mechanochemical conditions, a mineralization process enabling fluorine recovery as KF and K₂PO₃F for fluorination chemistry. The phosphate salts can be recovered for reuse, implying no detrimental impact on the phosphorus cycle. Therefore, PFASs are not only destructible but can now contribute to a sustainable circular fluorine economy.

Since the 1940s, anthropogenic perfluoroalkyl and polyfluoroalkyl substances (PFASs) have been produced for applications such as textile impregnation, firefighting foams, food packaging and cookware materials. Medical uses include implanted devices, orthopaedic components, catheters, pacemakers and surgical tools⁵. Structurally, PFASs feature multiple carbon–fluorine (C–F) bonds that account for their unique and valuable properties but are also responsible for their resistance to biological or chemical degradation¹. Today, environmental persistence and bioaccumulation have resulted in global PFAS contamination in drinking water, livestock and agricultural products, with evidence of a negative impact on human health upon chronic exposure^{6,7}. This state of play requires immediate action, including the development of PFAS removal approaches^{2–4} and responsible management of PFAS-contaminated waste streams^{8,9}. The PFAS degradation methods reported to date include chemical- and photochemical-initiated oxidation and reduction processes^{10–13}, mechanical^{14–24} and base-assisted destruction, including low-temperature mineralization^{25,26}, and incineration²⁷ among other techniques^{28,29} (Fig. 1a).

With the knowledge that all fluorochemicals are produced from fluorite^{30,31}, a naturally occurring mineral currently categorized as critical by the European Union and other countries, the availability of a mild method that destroys PFASs with recovery of the fluorine content for upcycling would represent a paradigm shift in PFAS management. Such an upcycling approach would contribute to diminishing the root cause of impending global challenges, such as resource shortages and uncertain supply chains linked to geopolitical turmoil. Here we disclose an operationally simple solution entailing the reaction of various PFAS classes with potassium phosphate salts applying mechanical energy. The process enables close to quantitative recovery of PFAS fluorine content as KF and K₂PO₃F. Because we demonstrated that K₂PO₃F can be

converted into KF or tetraalkylammonium fluorides, PFASs as diverse as polytetrafluoroethylene (PTFE; Teflon), polyvinylidene fluoride (PVDF), perfluorooctanoic acid (PFOA) or perfluorooctanesulfonic acid (PFOS) are not only destructible but can also serve as a viable fluorine source for upcycling into critically needed fluorochemicals for life and material sciences. This process enables the recovery of phosphate salts for reuse, which is an advantage in the era of phosphorus insecurity for fertilizer production (Fig. 1b).

Results and discussion

An observation made in the course of our study on the synthesis of fluorochemicals from fluor spar (CaF₂) served as a starting point of investigation³¹. We noted that ball milling CaF₂ with a phosphate salt (K₂HPO₄) in a stainless-steel jar with sealing rings made of PTFE (Teflon) instead of rubber gave higher yields of K₃(HPO₄)F and K_{2-x}Ca_y(PO₃F)_a(PO₄)_b, a new reagent for fluorination (Supplementary Information). This result suggests that fluoride leached from PTFE under these conditions, prompting the use of PTFE-free systems for CaF₂ chemistry. This outcome was unexpected because C–F bond cleavage is mechanistically distinct from an ion exchange process. Methods for repurposing fluoroplastics, such as PTFE, are limited^{12,32–34} and involve harsh reaction conditions³⁵; therefore, further investigation ensued (Fig. 2a). Ball milling PTFE with K₃PO₄ (1.25 equivalents (equiv.) per F) at 35 Hz for 3 h in a steel milling jar with a rubber sealing ring gave a solid material (PTFE mix^{KF}) for which the water-soluble fraction was analysed by ¹⁹F nuclear magnetic resonance (NMR) spectroscopy (10% D₂O in H₂O). Signals at –120.6 and –73.2 ppm (*J*_{PF} = 867 Hz) ascribed to F[–] (84%) and PO₃F^{2–} (15%), respectively, indicated near-quantitative fluorine recovery. Alternative phosphate salts, including K₂HPO₄, KH₂PO₄ and

¹Chemistry Research Laboratory, University of Oxford, Oxford, UK. ²Department of Chemistry, Colorado State University, Fort Collins, CO, USA. ³These authors contributed equally: Long Yang, Zijun Chen. ✉e-mail: robert.paton@colostate.edu; veronique.gouverneur@chem.ox.ac.uk

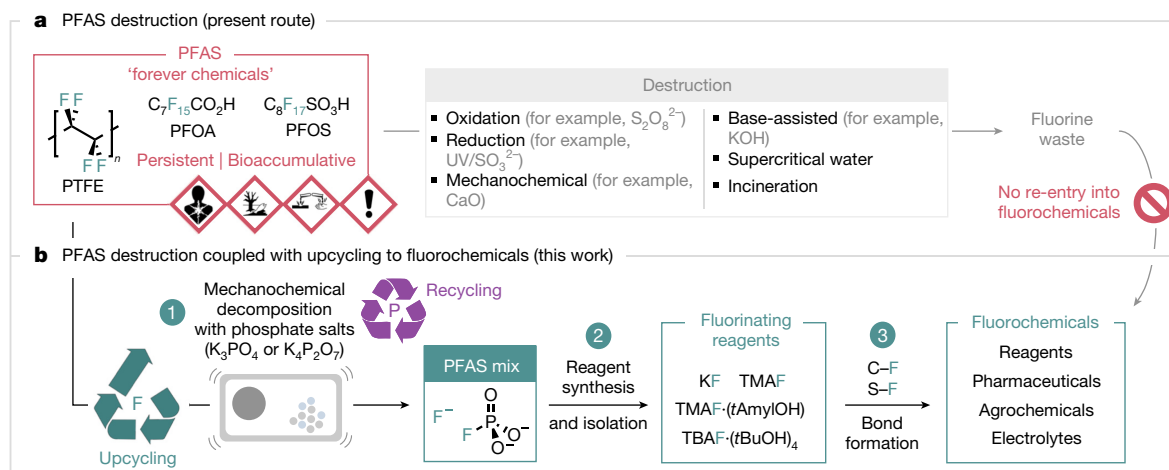


Fig. 1 | Synthesis of fluorochemicals from PFASs. a, Selection of existing routes for PFAS degradation. **b**, PFAS mineralization coupled with upcycling into essential fluorochemicals (this study). Credits: upcycling symbol in **b** adapted from <https://thenounproject.com/icon/upcycle-18167/>, under a

PDM1.0 licence (<https://creativecommons.org/publicdomain/mark/1.0/>); recycling symbol in **b** reproduced from <https://revvitysignals.com/products/research/chemdraw>.

$K_3P_3O_{10}$, were less effective, but $K_4P_2O_7$ stood out with the formation of a distinct mixture (PTFE mix^{PF}) for which ^{19}F NMR spectroscopy analysis (10% D_2O in H_2O) showed predominantly P–F bond formation (99% PO_3F^{2-} ; $\delta_F = -73.7$; $J_{PF} = 867$ Hz) and only trace amounts of F^- (less than 1%; $\delta_F = -120.1$). Replacing the steel components (milling jar and balls) with zirconia gave close to identical results, and a control experiment confirmed that PTFE degradation is induced by the phosphate salt under the reaction conditions and is not linked to metal leaching from the steel components. For comparison, KOH (1.25 equiv. per F), which is known to decompose PFOA and PFOS by applying mechanical energy^{14,16}, was found to be ineffective for releasing fluoride from PTFE (less than 10%) (Supplementary Information). These results prompted an in-depth investigation because potassium phosphate salts may offer a general and direct route to fluorinating reagents, such as KF , from PTFE and other PFASs, thereby contributing to a circular economy for the fluorochemical sector.

Further analysis gave useful information on the composition of PTFE mixes (Fig. 2b and Supplementary Information). Quantitative ^{31}P NMR spectroscopy (10% D_2O in H_2O) indicated that different ratios of PO_3F^{2-} , PO_4^{3-} , $P_2O_7^{4-}$ and $P_3O_{10}^{5-}$ were present in the PTFE mix^{KF} and PTFE mix^{PF}. For the PTFE mix^{KF}, $P_2O_7^{4-}$ ($\delta_P = -6.3$; 70% of total phosphorus (P_{tot})) was the predominant phosphorus species, followed by PO_4^{3-} ($\delta_P = 2.7$; 14% P_{tot}), PO_3F^{2-} ($\delta_P = 1.0$; $J_{PF} = 867$ Hz; 12% P_{tot}) and $P_3O_{10}^{5-}$ ($\delta_P = -5.5$; -20.3 ; $J_{PP} = 20$ Hz; 4% P_{tot}). In contrast, PO_3F^{2-} ($\delta_P = 1.5$; $J_{PF} = 867$ Hz; 79% P_{tot}) was the major species in the PTFE mix^{PF}, followed by PO_4^{3-} ($\delta_P = 2.9$; 14% P_{tot}), $P_3O_{10}^{5-}$ ($\delta_P = -5.5$; -19.5 ; $J_{PP} = 20$ Hz; 4% P_{tot}) and $P_2O_7^{4-}$ ($\delta_P = -6.3$; 3% P_{tot}). Quantitative ^{13}C NMR spectroscopy gave insights into the fate of the carbon skeleton. The water-soluble fraction of the PTFE mix^{KF} consisted mainly of CO_3^{2-} ($\delta_C = 165.5$; 48% C_{tot}), with trace amounts of $C_2O_4^{2-}$ ($\delta_C = 173.0$; 2% C_{tot}) and HCO_2^- ($\delta_C = 171.1$; 1% C_{tot}). For PTFE mix^{PF}, CO_3^{2-} ($\delta_C = 160.2$; 7% C_{tot}) was predominant, followed by $C_2O_4^{2-}$ ($\delta_C = 173.0$; 1% C_{tot}); HCO_2^- was not detected.

Taken together, these species accounted for only a fraction of the total carbon content of PTFE, prompting gas capture analysis. A significant quantity of CO_2 (42% C_{tot}) was released in the case of $K_4P_2O_7$ -induced PTFE degradation, but no CO_2 was detected with K_3PO_4 , which is an advantage in the era of decarbonization (Supplementary Information). The water-insoluble black solid isolated from the PTFE mix^{KF} and PTFE mix^{PF} was analysed using Raman spectroscopy. Bands at 1,355 and 1,579 cm^{-1} were observed, consistent with the disordered and graphitic bands of carbon (48% C_{tot} for both samples)³⁶. Solid-state ^{19}F , $^{19}F\{^{31}P\}$ and $^{31}P\{^{19}F\}$ NMR spectroscopy showed that the PTFE mix^{KF}

contains KF , $KF \cdot 2H_2O$, K_2PO_3F and $K_4P_2O_7$, whereas the PTFE mix^{PF} is mainly composed of K_2PO_3F . The presence of K_2PO_3F in the PTFE mix^{KF} and PTFE mix^{PF} with no residual PTFE was confirmed by powder X-ray diffraction analysis.

Control experiments were performed to further understand this solvent-free mechanochemical process (Extended Data Fig. 1a). Both K_3PO_4 and $K_4P_2O_7$ were subjected independently to ball milling in the absence of PTFE. No reactivity was observed for K_3PO_4 , but minor quantities of K_3PO_4 (3%) and $K_5P_3O_{10}$ (2%) were formed upon milling $K_4P_2O_7$ (Supplementary Information). We also investigated the ability of the PTFE degradation products K_2CO_3 , $K_2C_2O_4$, K_2PO_3F and $KHCO_2$ to decompose PTFE under otherwise similar ball milling conditions, demonstrating that K_2CO_3 was the most effective, yielding KF in 75%. These results indicate a complex mechanistic regime involving multiple oxyanion species. Further experiments demonstrated that ball milling K_2PO_3F with K_3PO_4 gave quantitative conversion to KF along with $K_4P_2O_7$; when ball milled with $K_4P_2O_7$, K_2PO_3F was mainly recovered, with 13% of KF being formed (Supplementary Information).

To gain insight into the ability of different oxyanions to decompose PTFE, we studied their global reactivity descriptors with $\omega B97xD/6-311++G(2d,2p)$ density functional theory (DFT) calculations (Extended Data Fig. 1b)³⁷. Specifically, the global nucleophilicity index N^{38-41} was calculated and compared against the total yield of mineralized products KF and K_2PO_3F . A positive correlation suggests nucleophilic behaviour of the oxyanions in the milling process (Extended Data Fig. 1b(i)). Alternative theoretical formulations of the nucleophilicity indices yielded consistent results (Supplementary Information). A putative nucleophilic substitution reaction between various oxyanions and the model PFAS perfluorobutane was therefore examined next (Extended Data Fig. 1b(ii)). The reaction with K_3PO_4 favoured an S_N2 transition structure at the internal carbon, with the lowest Gibbs free energy barrier ($\Delta G^\ddagger = 31.8$ kcal mol⁻¹). $K_4P_2O_7$ and K_2CO_3 gave the third and fourth lowest activation barriers ($\Delta G^\ddagger = 9.3$ and 10.4 kcal mol⁻¹ versus K_3PO_4 , respectively), demonstrating kinetic feasibility and the superiority of these three oxyanions for PFAS degradation. The ordering of computed activation barriers correlated with the experimental yields. For benchmarking, it is noteworthy that the weakest homolytic bond dissociation of perfluorobutane is 103 kcal mol⁻¹ (ref. 42), which is comparable to the average C–C bond energy of 90 kcal mol⁻¹ in PTFE^{43,44}. Because we experimentally determined the composition of the PTFE mix^{KF} (Fig. 2b), the standard enthalpy change (ΔH°) of an idealized process ($[C_2F_4]_n$ and K_3PO_4 leading to C , K_2CO_3 , KF and $K_4P_2O_7$; Supplementary

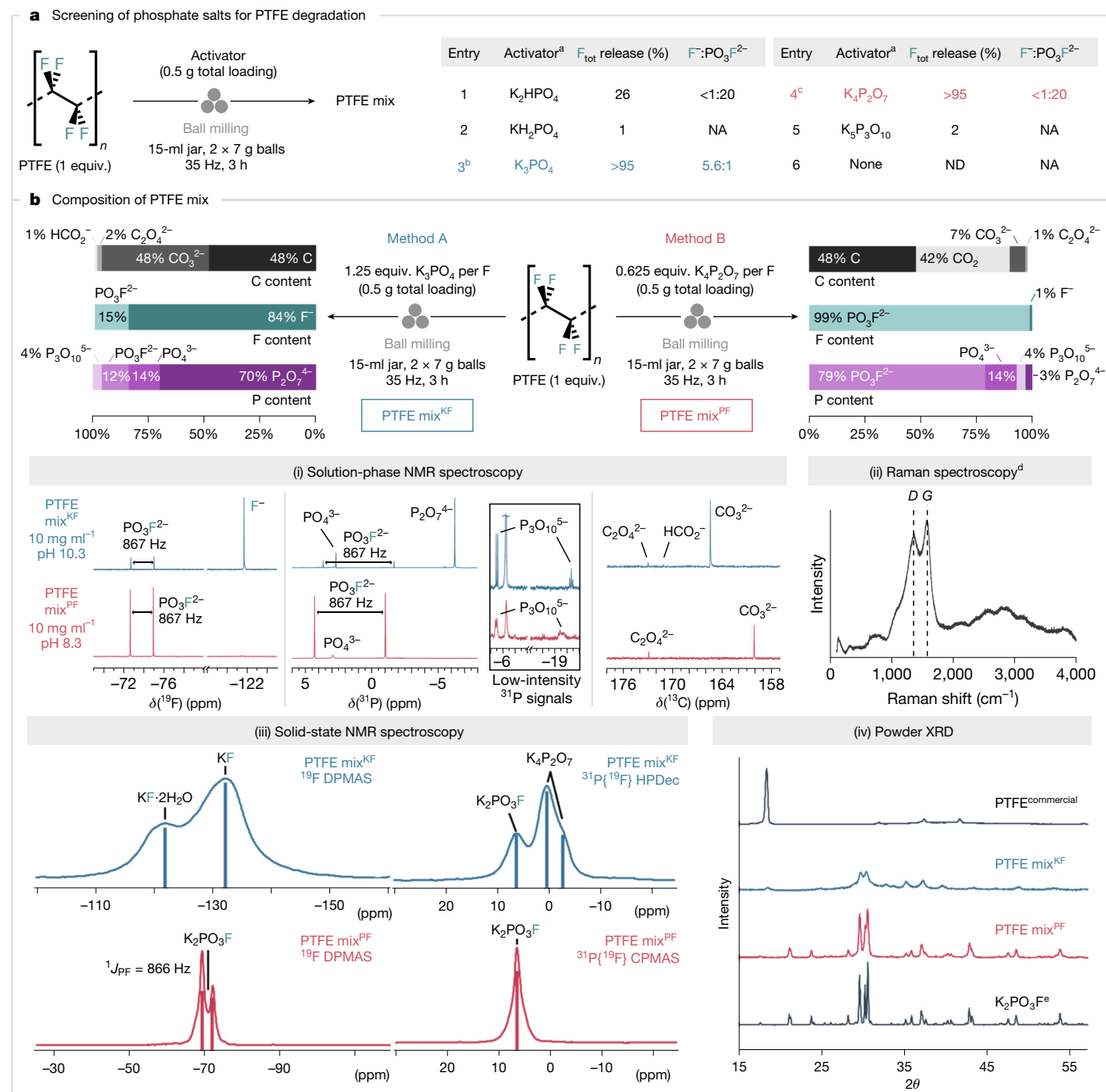


Fig. 2 | Phosphate-enabled mechanochemical mineralization of PTFE.

a, Screening of various phosphate salts as activators for PTFE. The total yield of released fluoride (both F⁻ and PO₃F²⁻) and their ratio were determined by quantitative ¹⁹F NMR spectroscopy (in 10% D₂O in H₂O using NaOTf as an internal standard). **b**, Identification of the C/F/P contents of PTFE mix by quantitative ¹³C/¹⁹F/³¹P NMR spectroscopy (in 10% D₂O in H₂O using KOAc or NaOTf as an internal standard) and Raman spectroscopy of water-insoluble black residue after aqueous extraction. Further analysis of PTFE mix by solid-state ¹⁹F/³¹P NMR

spectroscopy and powder X-ray diffraction (XRD). ^aActivator stoichiometry was kept constant at 1.25 equiv. P per F. ^bReaction was also performed in a 15-ml zirconia jar with 2 × 6 g zirconia balls affording 98% F_{tot} release (F⁻:PO₃F²⁻ = 5.5:1). ^cReaction was also performed in a 15-ml zirconia jar with 2 × 6 g zirconia balls affording 99% F_{tot} release (F⁻:PO₃F²⁻ <1:20). ^dThe observed bands are denoted as *D* (disordered carbon) and *G* (graphitic carbon). ^ePrepared mechanochemically from KF and KPO₃. NA, not applicable; ND, not detected.

Information) was determined as -143.5 kcal mol⁻¹. This compared to a value of -107.9 kcal mol⁻¹ for the decomposition of PTFE mix^{PF} ([C₂F₄]_n and K₄P₂O₇ leading to C, CO₂ and K₂PO₃F; Supplementary Information). The data are consistent with the favourable formation of KF (-2.95 eV per atom) and K₂PO₃F (-2.76 eV per atom) (Supplementary Information). Therefore, the phosphate-mediated decomposition of PTFE is enthalpically and entropically favourable.

The superiority of K₃PO₄ over KOH for the destruction of PTFE warrants further study of the solvation effect (that is, hydration). The putative S_N2 reaction of perfluorobutane at an internal carbon with anhydrous KOH has the second lowest Gibbs free energy barrier (ΔG[‡] = 34.3 kcal mol⁻¹) of all oxyanions investigated. However, as expected, for mono- and dihydrate clusters of KOH, nucleophilic substitution is a kinetically more demanding process in comparison

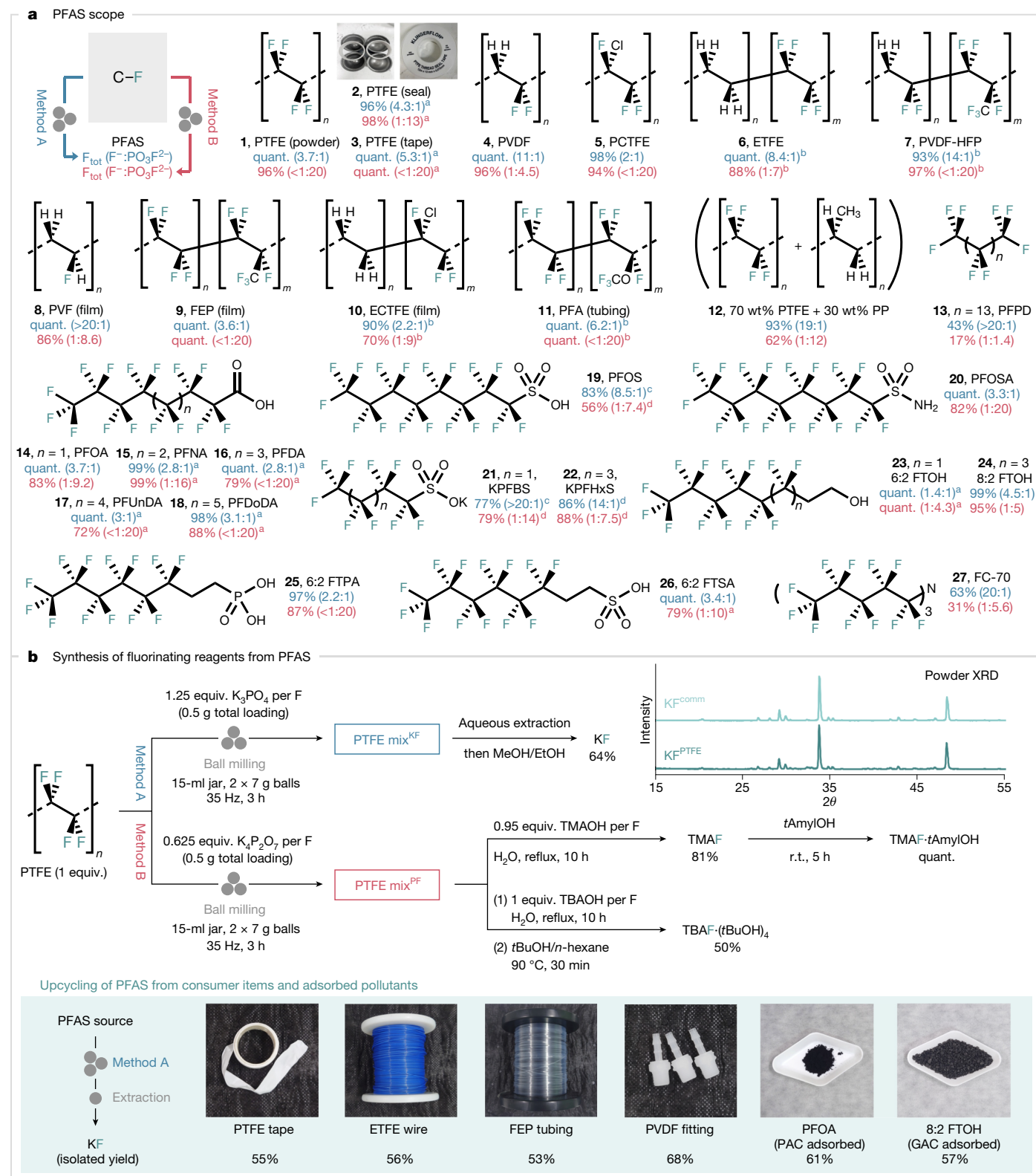


Fig. 3 | PFAS destruction and fluorinating reagents from PFAS. a, Scope of PFAS destruction. The total yield of released fluoride (both F^- and $PO_3F_2^-$) and their ratio were determined by quantitative ^{19}F NMR spectroscopy (in 10% D_2O in H_2O using $NaOTf$ as an internal standard). Reactions were performed in triplicates, and average yields are reported. **b**, Synthesis of KF and tetraalkylammonium fluoride from PTFE and other PFAS sources under

mechanochemical conditions. Yields of isolated products are reported. ^aReaction was performed once. ^bThe yield was calculated on the basis of the fluorine content of the copolymer as determined by elemental analysis. ^cThe amount of K_3PO_4 was increased to 2 equiv. per F. ^dReaction was carried out for 6 h. quant., quantitative; r.t., room temperature; TMAOH, tetramethylammonium hydroxide; TBAOH, tetrabutylammonium hydroxide.

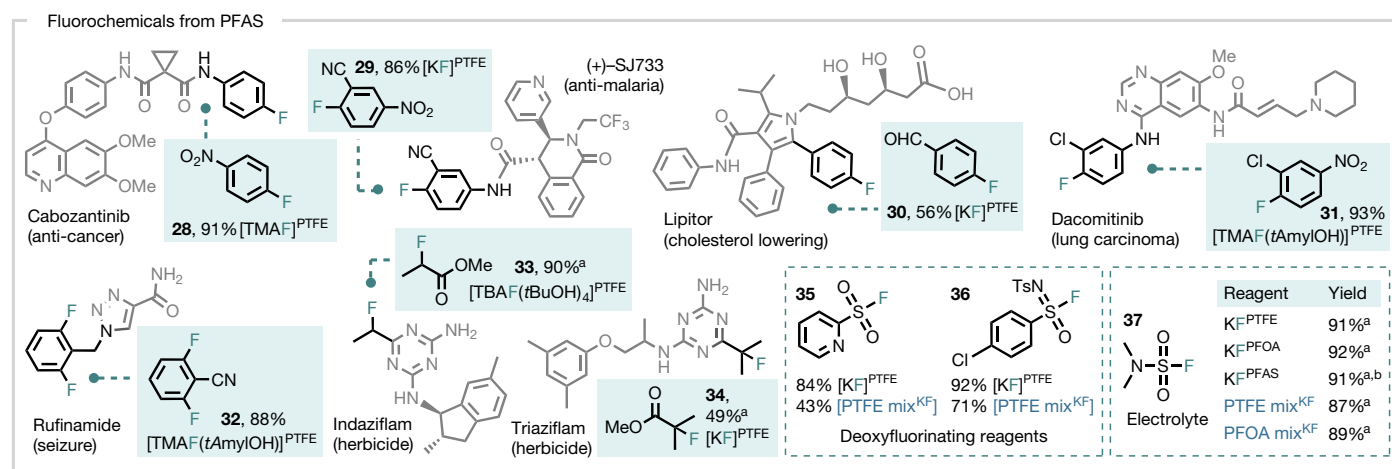


Fig. 4 | Synthesis of fluorochemicals from PFAS. Building block synthesis of high-value fluorochemicals using PFAS-derived fluorinating reagents (0.5-mmol scale unless otherwise stated). Yields of isolated products are reported. Detailed reaction conditions are stated in the Supplementary Information. ^aYield was determined by quantitative ¹⁹F NMR (in CDCl₃ using

4-fluoroanisole as an internal standard). ^bKF was isolated from a mixture of decomposed PFASs, including PFOS, PFOA, perfluoronanoic acid (PFNA), perfluorodecanoic acid (PFDA), PFOSA and 8:2 FTOH (Supplementary Information).

with anhydrous KOH ($\Delta\Delta G^\ddagger = 8.9$ and 16.3 kcal mol⁻¹, respectively). Such solvation effects also impact K₃PO₄ but to a lesser extent ($\Delta\Delta G^\ddagger = 5.5$ kcal mol⁻¹ (K₃PO₄·H₂O), 8.7 kcal mol⁻¹ (K₃PO₄·2H₂O) and 12.8 kcal mol⁻¹ (K₃PO₄·3H₂O)). Experimentally, inefficient PTFE decomposition was observed with KOH, irrespective of its water content (less than 10% fluoride release; Supplementary Information). By contrast, PTFE degradation was quantitative with anhydrous K₃PO₄, was poorly effective with K₃PO₄·H₂O (9% fluoride recovery) and did not occur with K₃PO₄·3H₂O. These data can be accounted for considering that the degradation of PTFE with KOH produces water, decreasing the hydroxide nucleophilicity through strong solvation as the reaction proceeds.

Having established the optimal conditions for the formation of fluoride and fluorophosphate from PTFE, we investigated the generality of this process with PFASs other than PTFE (Fig. 3a). The methodology was applied successfully to both polymeric (**1–12**) and non-polymeric PFASs (**13–27**); these include PTFE in various forms, including consumer Teflon seal and tape (**1–3**), PVDF (**4**), polychlorotrifluoroethylene (PCTFE) (**5**), ethylene tetrafluoroethylene (ETFE) (**6**), poly(vinylidene fluoride-co-hexafluoropropylene) (PVDF-HFP) (**7**), polyvinyl fluoride (PVF) film (**8**), fluorinated ethylene propylene (FEP) film (**9**), ethylene-chlorotrifluoroethylene (ECTFE) film (**10**), perfluoroalkoxy alkane (PFA) tubing (**11**), a mixture of polypropylene (PP) and

PTFE (**12**), perfluoropentadecane (PFPD) (**13**), PFOA (**14**), as well as long-chain derivatives (**15–18**), PFOS (**19**), perfluorooctanesulfonamide (PFOSA) (**20**), potassium perfluorobutanesulfonate (KPFBS) (**21**), potassium perfluorohexanesulfonate (KPFHxS) (**22**), 6:2 fluorotelomer alcohol (6:2 FTOH) (**23**), 8:2 fluorotelomer alcohol (8:2 FTOH) (**24**), 6:2 fluorotelomer phosphonic acid (6:2 FTPA) (**25**) and 6:2 fluorotelomer sulfonic acid (6:2 FTSA) (**26**). Noteworthy, the process also degraded FC-70 (**27**), which is a coolant liquid used in electronics.

With a general method to destroy PFAS, we developed an efficient route to isolate the PTFE-derived potassium fluoride (KF) (KF^{PTFE}) from the PTFE mix^{KF}. The extractive purification of PTFE mix^{KF} with H₂O and MeOH/EtOH enabled the isolation of KF^{PTFE} in 64% yield and 93% purity (calculated from PTFE; Supplementary Information). For comparison, the isolation of KF from PTFE ball milled with K₂CO₃ was more challenging and led to KF with lower yield (32%) and purity (55%). PTFE mix^{PF}, resulting from the activation of PTFE with K₄P₂O₇, served as the starting material for synthesizing tetramethylammonium fluoride (TMAF; 81% upon treatment with tetramethylammonium hydroxide (TMAOH)⁴⁵. TMAF was derivatized into its *tert*-amyl alcohol complex [TMAF·(*t*AmylOH)], a fluorinating reagent well documented for nucleophilic aromatic fluorination (S_NAr)⁴⁶. The bench-stable reagent tetrabutylammonium tetra(*tert*-butyl alcohol) fluoride [TBAF·(*t*BuOH)₄] (50%)

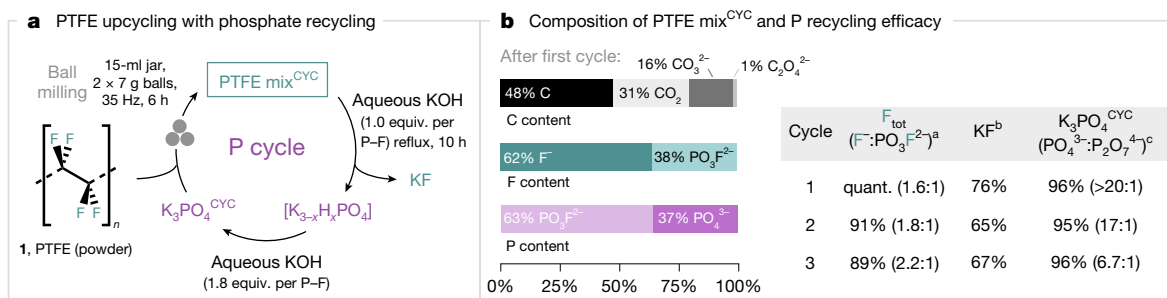


Fig. 5 | Phosphate recycling. **a**, Recovery of phosphate salts. **b**, Identification of C/F/P contents of PTFE mix^{CYC} after first cycle and efficacy of recovered phosphate salts. Ball milling conditions: PTFE (1 equiv.; 86 mg) milled with K₃PO₄ (0.625 equiv. per F; 457 mg) or K₃PO₄^{CYC} (457 mg) in a 15-ml stainless-steel milling jar, two chrome steel balls (2 × 7 g) at 35 Hz for 6 h. ^aThe total yield of released fluoride (F⁻ and PO₃F²⁻) as well as F⁻:PO₃F²⁻ ratio was determined by

quantitative ¹⁹F NMR spectroscopy (in 10% D₂O in H₂O using NaOTf as an internal standard). ^bYields for isolated KF are reported. ^cThe total yield of recovered phosphate (PO₄³⁻ and P₂O₇⁴⁻), as well as PO₄³⁻:P₂O₇⁴⁻ ratio was determined by quantitative ³¹P NMR spectroscopy (in 10% D₂O in H₂O using PO(OEt)₃ as an internal standard); recovered phosphate salts contain up to 8% carbonate.

was prepared in a similar manner⁴⁷. To demonstrate the applicability of this method, KF was successfully isolated from real-world consumer items, including PTFE tape, ETFE wire, FEP tubing and PVDF fittings. Furthermore, samples of PFAS adsorbed on powdered activated carbon (PAC) or granular activated carbon (GAC) were subjected to complete destruction, yielding KF for upcycling under identical conditions (Fig. 3b). All fluorinating reagents prepared from PTFE reacted as anticipated in the synthesis of various fluorochemical classes. KF^{PTFE} performed comparably to commercial KF (KF^{comm}) in substitution chemistry, leading to 2,4-dinitrofluorobenzene (Supplementary Information). It was used to prepare 2-fluoro-5-nitrobenzotrile (29) and methyl 2-fluoroisobutyrate (34), the precursors of (+)-SJ733 (anti-malaria) and triaziflam (herbicide), respectively. The deoxy-fluorinating reagents PyFluor (35) and SulfoxFluor (36), as well as the electrolyte dimethylsulfamoyl fluoride (37) were also prepared in good yields from KF^{PTFE} (Fig. 4). Notably, KF isolated from non-polymeric PFOA (KF^{PFOA}) and other PFAS (KF^{PFAS}), as well as crude mixtures (PTFE mix^{KF} and PFOA mix^{KF}) were efficient fluorinating reagents for S–F bond construction (35–37). The copper-mediated fluorination⁴⁸ of potassium 4-formylphenyltrifluoroborate (prepared from KF^{PTFE}) with KF^{PTFE} afforded 4-fluorobenzaldehyde (30), a precursor of LIPITOR (cholesterol-lowering drug)⁴⁹. Tetraalkylammonium fluoride reagents derived from PTFE mix^{PF} were used to access 4-fluoronitrobenzene (28), 2-chloro-1-fluoro-4-nitrobenzene (31), 2,6-difluorobenzotrile (32) and methyl 2-fluoropropanoate (33). These fluorochemicals are the precursors of cabozantinib (anti-cancer), dacomitinib (lung carcinoma), rufinamide (seizure) and indaziflam (herbicide) (Fig. 4).

With a technology relying on K₃PO₄ for PFAS destruction, we considered its possible environmental impact on the phosphorus cycle, including wastewater contamination and anthropogenic eutrophication⁵⁰. Therefore, our next goal was to establish that PTFE can be upcycled with a process enabling both the isolation of KF and the recovery of the phosphate salt for reuse (Fig. 5a). Because K₄P₂O₇ was identified as the predominant by-product of PTFE mix^{KF} and is itself an effective activator with formation of PTFE mix^{PF}, the quantity of K₃PO₄ was adjusted for PTFE destruction coupled with KF recovery and K₃PO₄ recycling. Specifically, milling PTFE with K₃PO₄ (0.625 equiv. per F) at 35 Hz for 6 h in a steel milling jar gave a solid material (PTFE mix^{CYC}) with quantitative fluorine release (F⁻:PO₃F²⁻ = 1.6:1), and no K₄P₂O₇ was observed by ³¹P NMR. PTFE mix^{CYC} was subjected to aqueous extraction to remove residual carbon black, followed by treatment with KOH (1 equiv. per P–F) at reflux for 10 h to ensure complete hydrolysis of K₂PO₃F. This process afforded KF isolated in 76% yield, along with K₃PO₄^{CYC} recovered (96% of total P content) after further treatment with aqueous KOH (1.8 equiv. per P–F). K₃PO₄^{CYC} is mainly composed of K₃PO₄ (85 wt%) along with traces of K₄P₂O₇ (4 wt%). The performance of the recycled K₃PO₄^{CYC} was maintained over two more cycles with effective KF and K₃PO₄ recovery (Fig. 5b).

Conclusion

In summary, this study presents a new approach to PFAS management, entailing a mineralization method coupled with the recovery of fluorine content for re-entry into the fluorochemical industry. This method stands out because it is applicable to all classes of PFAS, including harmful PFOA and the fluoroplastics PTFE and PVDF. The best results, both in terms of PFAS destruction and isolation of fluorinating reagents, were obtained by ball milling PFASs with potassium phosphate salts. These salts can be recovered for reuse; therefore, minimal impact is imposed on the longevity of finite phosphate rock reserves and the phosphorus cycle. Alternative oxyanions (including K₂CO₃) were competent but less effective, with the yield of fluoride release correlating with oxyanion nucleophilicity. This approach offers a route that not only controls the environmental impact of PFASs through highly effective mineralization, but it also contributes to the circularity of the fluorochemical industry.

Online content

Any methods, additional references, Nature Portfolio reporting summaries, source data, extended data, supplementary information, acknowledgements, peer review information; details of author contributions and competing interests; and statements of data and code availability are available at <https://doi.org/10.1038/s41586-025-08698-5>.

- Leung, S. C. E., Wanninayake, D., Chen, D., Nguyen, N.-T. & Li, Q. Physicochemical properties and interactions of perfluoroalkyl substances (PFAS)—challenges and opportunities in sensing and remediation. *Sci. Total Environ.* **905**, 166764 (2023).
- Meegoda, J. N., Bezerra de Souza, B., Casarini, M. M. & Kewalramani, J. A. A review of PFAS destruction technologies. *Int. J. Environ. Res. Public Health* **19**, 16397 (2022).
- Merino, N. et al. Degradation and removal methods for perfluoroalkyl and polyfluoroalkyl substances in water. *Environ. Eng. Sci.* **33**, 615–649 (2016).
- Verma, S., Lee, T., Sahle-Demessie, E., Ateia, M. & Nadagouda, M. N. Recent advances on PFAS degradation via thermal and nonthermal methods. *Chem. Eng. J. Adv.* **13**, 100421 (2023).
- Glüge, J. et al. An overview of the uses of per- and polyfluoroalkyl substances (PFAS). *Environ. Sci. Processes Impacts* **22**, 2345–2373 (2020).
- Hoskins, T. D. et al. Chronic exposure to a PFAS mixture resembling AFFF-impacted surface water decreases body size in northern leopard frogs (*Rana pipiens*). *Environ. Sci. Technol.* **57**, 14797–14806 (2023).
- Mikkonen, A. T. et al. Spatio-temporal trends in livestock exposure to per- and polyfluoroalkyl substances (PFAS) inform risk assessment and management measures. *Environ. Res.* **225**, 115518 (2023).
- Ateia, M., Alsaibee, A., Karanfil, T. & Dichtel, W. Efficient PFAS removal by amine-functionalized sorbents: critical review of the current literature. *Environ. Sci. Technol. Lett.* **6**, 688–695 (2019).
- Ilango, A. K. et al. Enhanced adsorption of mixtures of per- and polyfluoroalkyl substances in water by chemically modified activated carbon. *ACS ES&T Water* **3**, 3708–3715 (2023).
- Cui, J., Gao, P. & Deng, Y. Destruction of per- and polyfluoroalkyl substances (PFAS) with advanced reduction processes (ARPs): a critical review. *Environ. Sci. Technol.* **54**, 3752–3766 (2020).
- Khan, Q. et al. Advanced oxidation/reduction processes (AO/RPs) for wastewater treatment, current challenges, and future perspectives: a review. *Environ. Sci. Pollut. Res.* **31**, 1863–1889 (2024).
- Zhang, H., Chen, J.-X., Qu, J.-P. & Kang, Y.-B. Photocatalytic low-temperature defluorination of PFASs. *Nature* **635**, 610–617 (2024).
- Liu, X. et al. Photocatalytic C–F bond activation in small molecules and polyfluoroalkyl substances. *Nature* <https://doi.org/10.1038/s41586-024-08327-7> (2024).
- Zhang, K. et al. Destruction of perfluorooctane sulfonate (PFOS) and perfluorooctanoic acid (PFOA) by ball milling. *Environ. Sci. Technol.* **47**, 6471–6477 (2013).
- Zhang, Q., Lu, J., Saito, F. & Baron, M. Mechanochemical solid-phase reaction between polyvinylidene fluoride and sodium hydroxide. *J. Appl. Polym. Sci.* **81**, 2249–2252 (2001).
- Ateia, M., Skala, L. P., Yang, A. & Dichtel, W. R. Product analysis and insight into the mechanochemical destruction of anionic PFAS with potassium hydroxide. *J. Hazard. Mater. Adv.* **3**, 100014 (2021).
- Yang, N. et al. Solvent-free nonthermal destruction of PFAS chemicals and PFAS in sediment by piezoelectric ball milling. *Environ. Sci. Technol. Lett.* **10**, 198–203 (2023).
- Cagnetta, G. et al. Mechanochemical destruction of perfluorinated pollutants and mechanosynthesis of lanthanum oxyfluoride: a waste-to-materials process. *Chem. Eng. J.* **316**, 1078–1090 (2017).
- Turner, L. P. et al. Mechanochemical remediation of perfluorooctanesulfonic acid (PFOS) and perfluorooctanoic acid (PFOA) amended sand and aqueous film-forming foam (AFFF) impacted soil by planetary ball milling. *Sci. Total Environ.* **765**, 142722 (2021).
- Battye, N. J. et al. Use of a horizontal ball mill to remediate per- and polyfluoroalkyl substances in soil. *Sci. Total Environ.* **835**, 155506 (2022).
- Turner, L. P., Kueper, B. H., Patch, D. J. & Weber, K. P. Elucidating the relationship between PFOA and PFOS destruction, particle size and electron generation in amended media commonly found in soils. *Sci. Total Environ.* **888**, 164188 (2023).
- Battye, N. et al. Mechanochemical degradation of per- and polyfluoroalkyl substances in soil using an industrial-scale horizontal ball mill with comparisons of key operational metrics. *Sci. Total Environ.* **928**, 172274 (2024).
- Gobindlal, K., Shields, E., Whitehill, A., Weber, C. C. & Sperry, J. Mechanochemical destruction of per- and polyfluoroalkyl substances in aqueous film-forming foams and contaminated soil. *Environ. Sci.: Adv.* **2**, 982–989 (2023).
- Gobindlal, K., Zujovic, Z., Jaine, J., Weber, C. C. & Sperry, J. Solvent-free, ambient temperature and pressure destruction of perfluorosulfonic acids under mechanochemical conditions: degradation intermediates and fluorine fate. *Environ. Sci. Technol.* **57**, 277–285 (2023).
- Trang, B. et al. Low-temperature mineralization of perfluorocarboxylic acids. *Science* **377**, 839–845 (2022).
- Monsky, R. J., Li, Y., Houk, K. N. & Dichtel, W. R. Low-temperature mineralization of fluorotelomers with diverse polar head groups. *J. Am. Chem. Soc.* **146**, 17150–17157 (2024).
- Per- and Polyfluoroalkyl Substances (PFAS): Incineration to Manage PFAS Waste Streams* (US Environmental Protection Agency, 2020); www.epa.gov/sites/default/files/2019-09/documents/technical_brief_pfases_incineration_ioaa_approved_final_july_2019.pdf.
- Fang, J. et al. Treatment of per- and polyfluoroalkyl substances (PFAS): a review of transformation technologies and mechanisms. *J. Environ. Chem. Eng.* **12**, 111833 (2024).
- Berhanu, A. et al. A review of microbial degradation of per- and polyfluoroalkyl substances (PFAS): biotransformation routes and enzymes. *Sci. Total Environ.* **859**, 160010 (2023).

30. Harsanyi, A. & Sandford, G. Organofluorine chemistry: applications, sources and sustainability. *Green Chem.* **17**, 2081–2086 (2015).
31. Patel, C. et al. Fluorochemicals from fluorspar via a phosphate-enabled mechanochemical process that bypasses HF. *Science* **381**, 302–306 (2023).
32. Lee, J., Zhang, Q. & Saito, F. Synthesis of nano-sized lanthanum oxyfluoride powders by mechanochemical processing. *J. Alloys Compd.* **348**, 214–219 (2003).
33. Qu, J., He, X., Zhang, Q., Liu, X. & Saito, F. Decomposition pathways of polytetrafluoroethylene by co-grinding with strontium/calcium oxides. *Environ. Technol.* **38**, 1421–1427 (2017).
34. Sheldon, D. J., Parr, J. M. & Crimmin, M. R. Room temperature defluorination of poly(tetrafluoroethylene) by a magnesium reagent. *J. Am. Chem. Soc.* **145**, 10486–10490 (2023).
35. Améduri, B. & Hori, H. Recycling and the end of life assessment of fluoropolymers: recent developments, challenges and future trends. *Chem. Soc. Rev.* **52**, 4208–4247 (2023).
36. Saravanan, M., Ganesan, M. & Ambalavanan, S. An in situ generated carbon as integrated conductive additive for hierarchical negative plate of lead-acid battery. *J. Power Sources* **251**, 20–29 (2014).
37. Frisch, M. J. et al. Gaussian 16, Revision C.01 (Gaussian, Inc., 2016).
38. Domingo, L. R., Chamorro, E. & Pérez, P. Understanding the reactivity of captodative ethylenes in polar cycloaddition reactions. A theoretical study. *J. Org. Chem.* **73**, 4615–4624 (2008).
39. Domingo, L. R. & Pérez, P. The nucleophilicity N index in organic chemistry. *Org. Biomol. Chem.* **9**, 7168–7175 (2011).
40. Parr, R. G., Szentpály, L. V. & Liu, S. Electrophilicity index. *J. Am. Chem. Soc.* **121**, 1922–1924 (1999).
41. Chattaraj, P. K. & Maiti, B. Reactivity dynamics in atom–field interactions: a quantum fluid density functional study. *J. Phys. Chem. A* **105**, 169–183 (2001).
42. Dixon, D. A., Smart, B. E., Krusic, P. J. & Matsuzawa, N. Bond energies in organofluorine systems: applications to Teflon® and fullerenes. *J. Fluorine Chem.* **72**, 209–214 (1995).
43. Giannetti, E. Thermal stability and bond dissociation energy of fluorinated polymers: a critical evaluation. *J. Fluorine Chem.* **126**, 623–630 (2005).
44. Wu, E. C. & Rodgers, A. S. Kinetics of the gas phase reaction of pentafluoroethyl iodide with hydrogen iodide. Enthalpy of formation of the pentafluoroethyl radical and the π bond dissociation energy in tetrafluoroethylene. *J. Am. Chem. Soc.* **98**, 6112–6115 (1976).
45. Iashin, V., Wirtanen, T. & Perea-Buceta, J. E. Tetramethylammonium fluoride: fundamental properties and applications in C-F bond-forming reactions and as a base. *Catalysts* **12**, 233 (2022).
46. Morales-Colón, M. T. et al. Tetramethylammonium fluoride alcohol adducts for $S_{\text{N}}\text{Ar}$ fluorination. *Org. Lett.* **23**, 4493–4498 (2021).
47. Kim, D. W., Jeong, H.-J., Lim, S. T. & Sohn, M.-H. Tetrabutylammonium tetra(tert-butyl alcohol)-coordinated fluoride as a facile fluoride source. *Angew. Chem. Int. Ed.* **47**, 8404–8406 (2008).
48. Ye, Y., Schimmler, S. D., Hanley, P. S. & Sanford, M. S. $\text{Cu}(\text{OTf})_2$ -mediated fluorination of aryltrifluoroborates with potassium fluoride. *J. Am. Chem. Soc.* **135**, 16292–16295 (2013).
49. Zarganes-Tzitzikas, T., Neochoritis, C. G. & Dömling, A. Atorvastatin (Lipitor) by MCR. *ACS Med. Chem. Lett.* **10**, 389–392 (2019).
50. Jupp, A. R., Beijer, S., Narain, G. C., Schipper, W. & Slootweg, J. C. Phosphorus recovery and recycling—closing the loop. *Chem. Soc. Rev.* **50**, 87–101 (2021).

Publisher's note Springer Nature remains neutral with regard to jurisdictional claims in published maps and institutional affiliations.



Open Access This article is licensed under a Creative Commons Attribution 4.0 International License, which permits use, sharing, adaptation, distribution and reproduction in any medium or format, as long as you give appropriate credit to the original author(s) and the source, provide a link to the Creative Commons licence, and indicate if changes were made. The images or other third party material in this article are included in the article's Creative Commons licence, unless indicated otherwise in a credit line to the material. If material is not included in the article's Creative Commons licence and your intended use is not permitted by statutory regulation or exceeds the permitted use, you will need to obtain permission directly from the copyright holder. To view a copy of this licence, visit <http://creativecommons.org/licenses/by/4.0/>.

© The Author(s) 2025

Data availability

All data are in the Supplementary Information or are available from the corresponding authors upon request.

Acknowledgements We thank N. Rees for acquiring solid-state NMR spectra, A. Thompson for fruitful discussions and the University of Oxford Advanced Research Computing facility (<https://doi.org/10.5281/zenodo.22558>). This research was funded by the European Research Council (agreement no. 832994 to L.Y., T.S., C.A.G. and V.G.), the EU Horizon 2020 Research and Innovation Programme through a UKRI Postdoctoral Fellowships Guarantee (EP/X02458X/1 to L.Y.), the Engineering and Physical Sciences Research Council (EP/V013041/1 to Z.C.), the Austrian Science Fund (FWF) (J 4705 to T.S.) and the National Science Foundation (CHE-2400056 to R.S.P.).

Author contributions L.Y. and Z.C. contributed equally to this study. V.G. conceived and directed the study. L.Y., Z.C., C.A.G. and T.S. designed and performed the experiments.

L.Y., Z.C., C.A.G., T.S. and V.G. analysed the experimental data. Z.C. performed the quantum chemical calculations. Z.C. and R.S.P. analysed the computational data. The Article was written by V.G. with contributions from all authors.

Competing interests A patent has been filed that may provide royalties to L.Y., Z.C., C.A.G., T.S. and V.G. (GB 2410558.7).

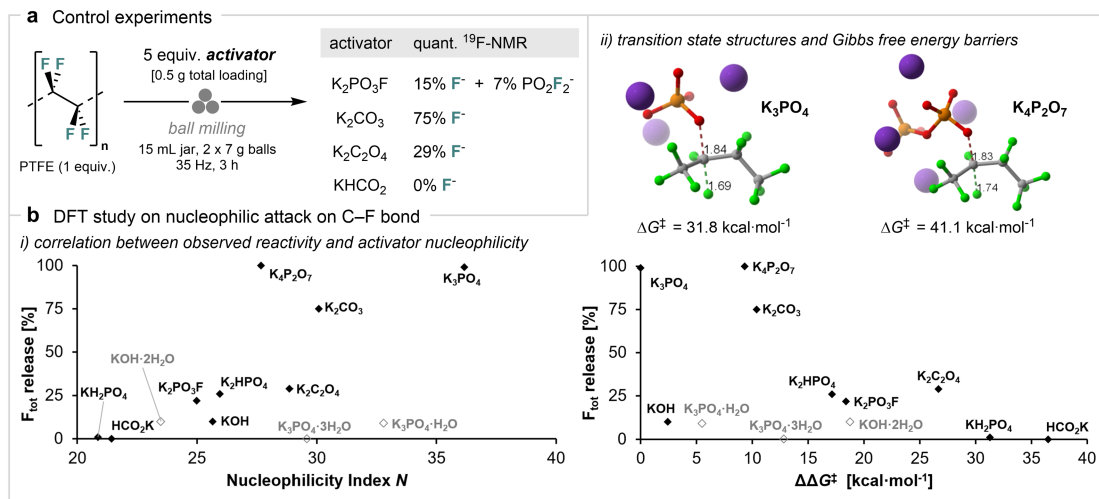
Additional information

Supplementary information The online version contains supplementary material available at <https://doi.org/10.1038/s41586-025-08698-5>.

Correspondence and requests for materials should be addressed to Robert S. Paton or Véronique Gouverneur.

Peer review information *Nature* thanks the anonymous reviewers for their contribution to the peer review of this work.

Reprints and permissions information is available at <http://www.nature.com/reprints>.



Extended Data Fig. 1 | Control experiments and DFT study. **a**, Control experiments employing by-products as activators for PTFE. Yields of F^- and PO_2F_2^- were determined by quantitative ^{19}F NMR spectroscopy (in 10% D_2O in H_2O using NaOTf as an internal standard). **b**, DFT computational studies showing a

correlation between observed reactivity and (i) oxyanion nucleophilicity parameter as well as an inverse correlation with (ii) $\text{S}_{\text{N}}2$ barrier height; hydrated salts are shown in grey.